

Proton Transfer in Matrix-Isolated 3-Hydroxyflavone and 3-Hydroxyflavone Complexes

G. A. Brucker and D. F. Kelley*

Department of Chemistry, Colorado State University, Fort Collins, Colorado 80523
(Received: November 21, 1986)

The proton-transfer dynamics of 3-hydroxyflavone (3HF) and 3HF-solvent complexes have been studied in 10 K argon matrices. Both static and picosecond fluorescence spectroscopies were used. The results indicate that proton transfer in bare molecules occurs quite rapidly (<10 ps). The 3HF-solvent complexes are formed by codeposition of argon:solvent mixtures (typically 2000:1) with 3HF followed by matrix annealing. Solvents include water, methanol, ethanol, and diethyl ether. The results show that proton transfer is very fast (<10 ps) in alcohol and water monosolvates and can be interpreted in terms of cyclically hydrogen-bonded structures. The results also show that the diethyl ether monosolvate undergoes proton transfer in about 40 ps. Solvation with two or more waters or alcohols was found to inhibit proton transfer.

Introduction

Proton-transfer reactions have been extensively studied for many years and occupy an important role in chemistry. The study of proton-transfer reactions is facilitated when both acid and base moieties are on the same molecule. In general it is found that photoexcitation increases the acidity of aromatic alcohols and the basicity of aromatic ketones.¹ In many molecules this results in an energetically favorable excited-state proton-transfer (ESPT) reaction. 3-Hydroxyflavone (3HF) is an extensively studied molecule which exhibits ESPT. Excited-state proton transfer in 3HF was first proposed by Sengupta and Kasha² to explain the dual blue and green luminescence. In their original paper they describe the behavior of 3HF in hydrocarbon solvents in terms of excited-state intramolecular proton transfer along the intramolecular hydrogen bond and make the first reference to the effects that breaking that intramolecular hydrogen bond could have on the ESPT process. The mechanism of proton transfer in 3HF is shown in Scheme I.

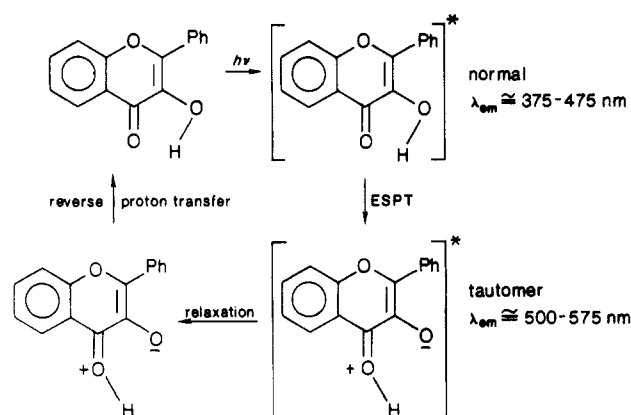
Studies by Woolfe and Thistlethwaite³ described the effects of viscosity, solvent, and temperature on ESPT. The behavior of 3HF in MeOH was explained in terms of two 3HF-methanol complexes: a cyclically hydrogen-bonded monosolvate which undergoes proton transfer and a disolvate which does not.

The subsequent work of Barbara et al.⁴ reported picosecond kinetic behavior for both the normal molecule emission decay and the tautomer emission risetime in several solvents (hydrocarbons, alcohols, ether, etc). Several models were presented in order to describe the observed kinetics, but no general model which would be applicable to all solvents could be developed for ESPT in this molecule. Itoh et al.⁵ has also reported normal and tautomeric emission kinetics and two-step laser excitation studies of 3HF in several solvents. These authors conclude that in hydrocarbon solvents, ESPT occurs slowly (tens to hundreds of picoseconds) and that phenyl rotation is strongly coupled to the proton-transfer event. The two-step laser excitation studies were interpreted in terms of slow (microseconds) reverse proton transfer in aprotic solvents.

Recently, McMorrow and Kasha⁶ have performed solvent dilution studies which show that the observation of normal molecule emission and the corresponding biexponential kinetics observed in hydrocarbon solvents were due to the presence of trace quantities of hydrogen-bonding impurities. In rigorously purified and dried hydrocarbon solutions the blue (normal) luminescence is absent at all temperatures. The static spectroscopic results obtained in other solvents were also interpreted in terms of different 3HF-solvent complexes and the competition between intra- and intermolecular hydrogen bonding. The above studies show that the nature of the solvent environment dramatically affects the 3HF ESPT dynamics.

In this paper we report the production and spectroscopic characterization of rare-gas matrix-isolated hydrogen-bonded

SCHEME I



solute-(solvent)_n, $n = 0, 1, 2$, complexes. Complexes formed in this environment in many cases maintain sharp, well-resolved spectral lines and can be selectively excited and detected. We have found that methanol, ethanol, diethyl ether, and water complexes can be readily formed with many different solutes in 10 K argon matrices.

The complexes are formed by codeposition of dilute solvent/argon mixtures, with very low concentrations of the solute, on a brass block at 10 K. Subsequent annealing of the matrix results in the desired solute-(solvent)_n, $n = 1, 2, \dots$, complexes. The annealing temperature is chosen such that solvent diffusion is facile, but the solutes are immobile. This technique is quite general, and the only restriction on the solute is that it must be at least very slightly volatile. The phenomenon of vastly different diffusion rates for small and large molecules in matrices has been well known for many years, and similar techniques have previously been used to generate monosolvate complexes.⁷ Matrix isolation

(1) Vander Donckt, E. *Prog. React. Kinet.* **1970**, *5*, 273. Ireland, J. F.; Wyatt, P. A. H. *Adv. Phys. Org. Chem.* **1976**, *12*, 131.

(2) Sengupta, P. K.; Kasha, M. *Chem. Phys. Lett.* **1979**, *68*, 382.

(3) Woolfe, G. J.; Thistlethwaite, P. J. *J. Am. Chem. Soc.* **1981**, *103*, 6916.

(4) (a) Strandjord, A. J. G.; Courtney, S. H.; Friederich, D. M.; Barbara, P. F. *J. Phys. Chem.* **1983**, *87*, 1125. (b) Strandjord, A. J. G.; Barbara, P. F. *Chem. Phys. Lett.* **1983**, *98*, 21. (c) Strandjord, A. J. G.; Barbara, P. F. *J. Phys. Chem.* **1985**, *89*, 2255. (d) Strandjord, A. J. G.; Smith, D. E.; Barbara, P. F. *J. Phys. Chem.* **1985**, *89*, 2365. (e) Barbara, P. F.; Strandjord, A. J. G. In *Ultrafast Phenomena*, Auston, D. H., Eisinger, K. B., Ed.; Springer-Verlag: Berlin, 1984.

(5) (a) Itoh, M.; Fujimara, Y. *J. Phys. Chem.* **1983**, *87*, 4558. (b) Itoh, M.; Tokamura, K.; Tanimoto, Y.; Okada, Y.; Takeuchi, H.; Obi, K.; Tanaka, I. *J. Am. Chem. Soc.* **1982**, *104*, 4164. (c) Itoh, M.; Tanimoto, Y.; Tokamura, K. *J. Am. Chem. Soc.* **1983**, *105*, 3339. (d) Itoh, M.; Furiwara, Y.; Sumitani, M.; Yoshihara, K. *J. Phys. Chem.* **1986**, *90*, 5672.

(6) (a) McMorrow, D.; Kasha, M. *J. Am. Chem. Soc.* **1983**, *105*, 5133. (b) McMorrow, D.; Kasha, M. *J. Phys. Chem.* **1984**, *88*, 2235. (c) McMorrow, D.; Kasha, M. *Proc. Natl. Acad. Sci. U.S.A.* **1984**, *81*, 3375.

(7) (a) Sass, C. S.; Ault, B. S. *J. Phys. Chem.* **1986**, *90*, 4533. (b) Ault, B. S. *J. Am. Chem. Soc.* **1978**, *100*, 2426.

* Alfred P. Sloan Fellow.

techniques have also been used to trap hydrated solute complexes formed in the gas phase.⁸ We have used this matrix annealing technique to produce $3\text{HF}\cdot(\text{solvent})_n$, $n = 1, 2$, complexes. By means of steady-state spectroscopy it is possible to detect and characterize $3\text{HF}\cdot(\text{ROH})_n$, $n = 1, 2$, complexes, for $R = \text{H, Me, Et}$. We have also studied $3\text{HF}\cdot\text{Et}_2\text{O}$ complexes. Picosecond emission spectroscopy was used to study ESPT in each of these complexes.

Experimental Section

The matrix isolation system is based on an Air Products 202E closed-cycle displax. The displax and vacuum system were pumped by a 3-in. Blazars turbomolecular pump. Base pressures of 10^{-7} Torr were easily obtained. Argon matrices were deposited at a rate of ~ 10 Torr cm^3/s on a brass block maintained at either ~ 10 or 30 K. Deposition times were typically 1 h. The argon used was high purity ($>99.998\%$) and dried by passage through a liquid nitrogen trap.

3-Hydroxyflavone (Aldrich) was purified by repeated resublimation under high vacuum. The surface onto which condensation occurred during the resublimations was maintained at ~ 50 °C. This resulted in a minimum amount of water condensing with the 3HF. The 3HF was further dried by high vacuum pumping for at least 1 h prior to deposition. Deuteriation was accomplished by extracting 3-deuterioxyflavone (3DF) in ether from D_2O . Following several extractions, the ether/3DF solution was transferred to the high-vacuum system where the ether and any remaining D_2O was pumped off. This was followed by several resublimations at high vacuum to ensure the complete removal of all ether and D_2O . The purified dry 3HF was sublimed into the argon stream at 55 °C immediately prior to 3HF/Ar condensation on the cold (10 or 30 K) brass block. The resulting 3HF/Ar (no solvent) matrices were very pure and extremely dry.

Matrix-isolated $3\text{HF}\cdot(\text{solvent})_n$ complexes were produced by condensing 3HF with argon/solvent gas mixtures at 10 K. Typical argon:solvent mixing ratios were 2000:1. This results in very little complex formation upon deposition. Subsequent heating (annealing) of the matrix to 26–30 K results in slow diffusion of the solvents, producing the desired $3\text{HF}\cdot(\text{solvent})_n$ complexes on the tens of minutes time scale. In some cases 3HF/Ar/solvent mixtures were deposited at 30 K resulting in complex formation during deposition.

The methanol used was spectral grade and was dried by distillation over magnesium methoxide, generated in-situ by reaction with iodine-activated magnesium metal. A similar procedure was used with ethanol. The ether was anhydrous reagent ($\text{H}_2\text{O} < 0.002\%$) and used without further purification.

The light source used for the steady-state spectra was a 150-W Xe lamp (fluorescence excitation) or a 200-W Hg/Xe lamp (dispersed emission) and a $1/8$ M double monochromator (Oriel) with 1200 grooves/mm gratings (resolution 0.5 nm). Dispersed emission spectra were collected with a 0.64 M ISA monochromator with a 1200 grooves/mm grating (resolution ~ 0.2 Å). The detector was a Hamamatsu R943-02 Ga-As PMT with single-photon-counting electronics. All spectra reported here are uncorrected.

The apparatus used in the time-resolved measurements was based on an active/passive mode-locked Nd:YAG laser. Sample excitation was with the third harmonic (355 nm) 25-ps, 0.02-mJ pulses focused to about a 1-mm-diameter spot size. In some cases excitation was provided with 364-nm pulses generated by stimulated rotational Raman scattering of circularly polarized 355-nm pulses focused into 15 atm of hydrogen. The 364-nm excitation pulse widths and power densities were comparable to those used with 355-nm pulses. Time-resolved detection was accomplished with a Hamamatsu C979 streak camera. The streak camera was coupled to a PAR 1254E SIT Vidicon and interfaced to a DEC

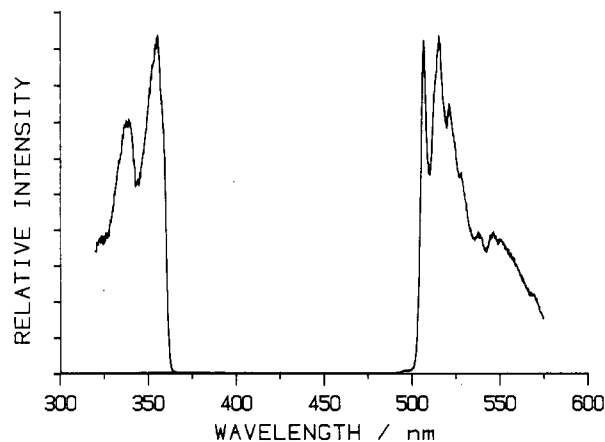


Figure 1. Fluorescence excitation and dispersed emission spectra of 3HF in 10 K argon. Expansion of the ordinate shows no detectable emission in the 400–450-nm region.

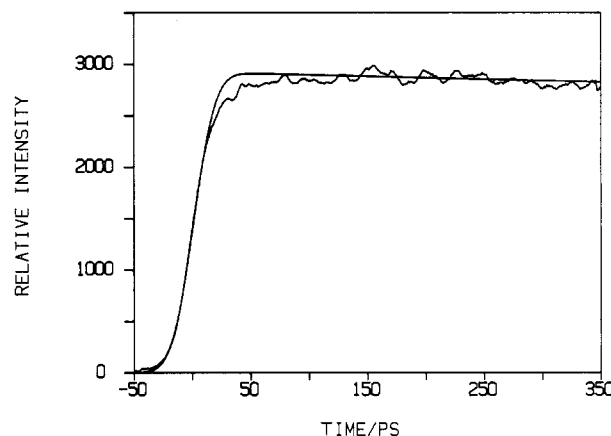


Figure 2. Tautomeric emission kinetics of unsolvated 3HF in 10 K argon following 355-nm picosecond excitation. The observation wavelength was 550 ± 30 (fwhm) nm. Also shown is a calculated curve corresponding to the convolution of the instrument response function and a fast risetime.

LSI 11/02 computer. Wavelength selection was accomplished by a Spex $1/4$ M monochromator with a 600 grooves/mm grating. The spectral bandpass was typically ~ 4 nm. The monochromator introduces some temporal dispersion, and the temporal instrument response function was ~ 35 ps (full width at half-maximum). Accurate determination of the temporal instrument response function results in actual temporal resolution considerably better than 35 ps.

Results and Discussion

Unsolvated 3HF. 1. Excited-State Proton Transfer. The dispersed emission and fluorescence excitation spectra of 3HF in a pure dry argon matrix deposited at 10 K is shown in Figure 1. The lowest singlet excited state is known to be (π, π^*) in nature, with the carbonyl (n, π^*) state at higher energy. Analysis of these spectra can provide significant information about the potential surfaces on which proton transfer occurs. The 0_0^0 line of the dispersed emission spectrum is Stokes shifted ~ 8000 cm^{-1} from that of the excitation spectrum. Previous studies²⁻⁶ have shown that this spectrally shifted emission is from the tautomeric form of the molecule formed by ESPT as indicated in Scheme 1. Figure 1 shows that no normal emission is detected. This observation, along with the assumption of comparable oscillator strengths of the normal and tautomeric forms, allows us to put an upper limit of a few picoseconds on the proton-transfer time.

The tautomeric emission kinetics of bare, matrix-isolated, 10 K 3HF following 355-nm excitation are shown in Figure 2. The vast majority of the tautomeric emission risetime is limited by the instrument temporal response, indicating that proton transfer occurs in < 10 ps. A small fraction ($\sim 10\%$) of the tautomeric emission in Figure 2 shows a finite risetime. The time-resolved

(8) (a) Nelander, B. *J. Chem. Phys.* **1978**, *69*, 3870. (b) Nelander, B. *J. Chem. Phys.* **1980**, *72*, 77. (c) Nelander, B.; Nord, L. *J. Phys. Chem.* **1982**, *86*, 4375. (d) Engdahl, A.; Nelander, B. *Chem. Phys. Lett.* **1983**, *100*, 129. (e) Engdahl, A.; Nelander, B. *Chem. Phys. Lett.* **1985**, *113*, 49. (f) Engdahl, A.; Nelander, B. *J. Phys. Chem.* **1985**, *89*, 2860.

results reported here were obtained with wavelength selection provided by a 550 ± 30 nm (full width at half-maximum) interference filter. Thus, almost the entire tautomeric band was observed, with greatest sensitivity at 550 nm. We note that experiments with finer wavelength resolution show considerable evolution of the tautomeric spectrum in the first ~ 100 ps. Specifically, the kinetics of vibrationally unrelaxed tautomeric emission (485–495 nm) show entirely fast risetimes, confirming that all ESPT takes place very rapidly. This spectral evolution is due to vibrational relaxation and/or phenyl rotation following proton transfer and will be discussed in a later paper.¹⁰ These results are consistent with the complete lack of detectable normal emission with both the static spectrometer and the streak camera. This very fast ESPT rate at 10 K indicates that there is no intrinsic barrier to proton transfer, or that tunneling through the barrier is quite facile.

The above static and time-resolved results are inconsistent with the recent results of Aartsma et al.,⁹ which report a tautomeric risetime of ~ 40 ps in low temperature hydrocarbon glasses. They are also inconsistent with the recent results of Itoh et al.,^{5d} which report biphasic tautomer risetimes. Itoh et al.^{5d} report fast and slow tautomeric emission risetimes of 60 and 287 ps, respectively, in 192 K 3-methylpentane solutions. The spectral evolution mentioned above may explain part of the discrepancy between these results and those reported in ref 9 and 5d.

Line width measurements of fluorescence excitation spectra can often provide lower limits on state lifetimes. However, in this case, analysis of the fluorescence excitation spectrum is somewhat ambiguous. Figure 1 shows that little or no vibrational structure can be resolved. Deposition of 3HF/argon onto a 30 K block results in a far more uniform matrix than those obtained by 10 K deposition, presumably with fewer types of guest sites. This often reduces the extent of inhomogeneous broadening. However, matrices deposited at 30 K yield very similar unresolved fluorescence excitation spectra. The lack of resolved vibrational structure may be due to homogeneous broadening caused by very rapid proton transfer, or due to vibronic spectral congestion and/or inhomogeneous broadening. The excitation spectrum obtained from 3DF is quite similar to that of 3HF. The lack of a large spectral shift upon deuteration indicates that OH stretch frequency is approximately the same in the ground and excited states. The lack of any ESPT barrier would result in very large excited-state proton motions and low vibrational frequencies. As a result, the excited state OH and OD stretch zero point energies would be much closer than in the ground state, resulting in a considerable blue-shift of the 0_0^0 line upon deuteration. The approximate coincidence of the 3HF and 3DF 0_0^0 transitions therefore implies the existence of an energetic barrier to ESPT. However, we stress that, in the absence of resolved spectra, we cannot unambiguously determine whether or not there exists an energetic barrier to ESPT in the isolated molecule.

2. Reverse (Ground-State) Proton Transfer. Higher resolution reveals no fine structure in either the fluorescence excitation or dispersed emission spectra beyond what is seen in Figure 1. The dispersed emission spectrum has its origin at 506.3 nm ($19\,750\text{ cm}^{-1}$) and shows vibrational bands at ~ 245 (shoulder), 332, 573, 816, ~ 1200 , and $\sim 1450\text{ cm}^{-1}$ with respect to that origin. Deuteration of the hydroxyl results in a $\sim 15\text{-cm}^{-1}$ red shift in the origin, but no detectable change in the coarse vibronic structure. This lack of hydrogen motion activity in the spectrum indicates that the equilibrium OH bond distance does not change dramatically between the ground- and excited-state tautomer. Furthermore, the modest (15 cm^{-1}) shift in the 0_0^0 line upon deuteration indicates that OH force constants are only slightly reduced in the ground- compared to excited-state tautomers.

As indicated above, matrix deposition onto a 30 K block often reduces the extent of inhomogeneous broadening. 3HF and 3DF dispersed emission spectra following 30 K deposition are shown

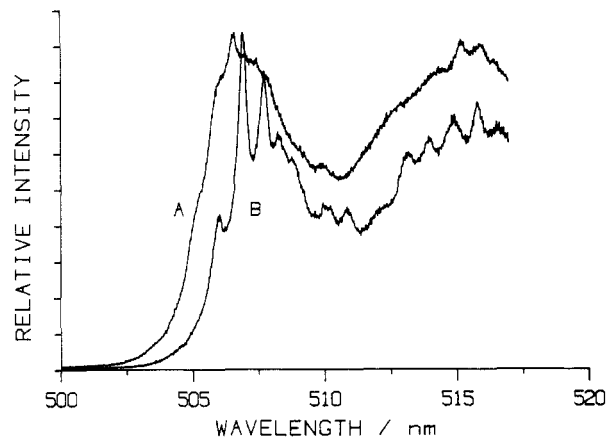


Figure 3. Dispersed emission spectra of (A) 3HF and (B) 3DF in argon matrices deposited at 30 K. The excitation wavelength was 355 nm.

in Figure 3. These spectra show many partially resolved, closely spaced peaks. Figure 3 shows that this spectral sharpening is much more pronounced in 3DF than in 3HF. Variation of the excitation wavelength changes the relative intensities of these peaks, indicating that they correspond to different sites in the matrix. The high-resolution spectrum has the same coarse structure as the 10 K deposition spectrum shown in Figure 1. The fine structure due to resolved sites is very complicated, and no attempt to analyze it will be made.

Although the dispersed emission lines are not completely resolved, it is possible to estimate a 0_0^0 line width for each site in the matrix of about 20 cm^{-1} for 3DF. The 3HF line width can be estimated to be roughly 90 cm^{-1} . A lower limit to the reverse proton and deuteron transfer rate can be obtained from the dispersed emission line widths: $\tau = (2\nu_{1/2}\pi c)^{-1}$. This line width indicates that the reverse proton (deuteron) transfer requires at least 60 fs (260 fs) following population of the ground-state tautomer. If there were no barrier to reverse proton transfer, then this would occur on the time scale of an OH stretch motion, about 10 fs. The dispersed emission spectrum therefore establishes that the ground-state potential surface has two minima, corresponding to the normal and tautomeric forms. Furthermore, we expect deuteration to have only a slight effect on the inhomogeneous component of the dispersed emission line widths. The difference between the observed 3HF and 3DF line widths may therefore be a result of different homogeneous line widths and may reflect differences in ground-state tautomer lifetimes. (We note that in both cases the excited-state tautomer lifetime is quite long and does not contribute significantly to homogeneous broadening.) If this interpretation is correct, then inhomogeneous widths are quite small ($\lesssim 20\text{ cm}^{-1}$) implying that the reverse proton transfer time in 3HF is close to that calculated from the line width (~ 60 fs). This is consistent with recent time-resolved stimulated emission pumping results¹¹ which indicated a reverse proton transfer time of less than 30 ps. However, we emphasize that line width measurements only give unambiguous lower limits of state lifetimes. It is possible that other inhomogeneous broadening mechanisms may contribute to the 3HF line widths, and the ground-state tautomer may have a lifetime much greater than the 60 fs calculated on the basis of purely homogeneous broadening.

Spectra and ESPT Dynamics of 3HF Complexes. **1. Assignment of Stoichiometries.** Codeposition of 3HF with an argon:solvent gas mixture (2000:1) results in spectra which are quite similar to those shown in Figure 1. Subsequent annealing of the matrix results in diffusion of the solvent molecules. The temperature at which solvent diffusion becomes appreciable varies with the size of the solvent molecules. For example, at 28–30 K, methanol will diffuse through the matrix, on the tens of minutes time scale. Diffusion initially results in the production of $3\text{HF}\cdot(\text{MeOH})_1$ complexes. As the $3\text{HF}\cdot(\text{MeOH})_1$ concentration

(9) McMorow, D.; Dzugan, T. P.; Aartsma, T. *J. Chem. Phys. Lett.* **1984**, 103, 492.

(10) Brucker, G. a.; Kelley, D. F., to be published.

(11) Dzugan, T. P.; Schmidt, J.; Aartsma, T. *J. Chem. Phys. Lett.* **1986**, 127, 336.

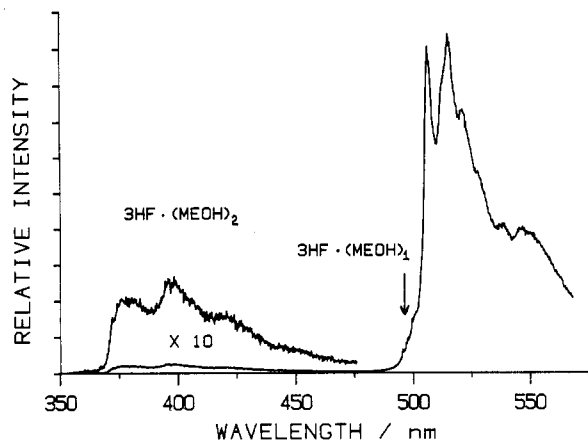


Figure 4. Dispersed emission spectra of 3HF in an argon:methanol matrix (2000:1). The excitation wavelength was 355 nm following 15 min of annealing at 30 K. The 400–450- and 495-nm features were almost completely absent prior to annealing.

increases subsequent methanol diffusion will produce a certain amount of $3\text{HF}\cdot(\text{MeOH})_2$ complexes. $(\text{MeOH})_n$, $n \geq 2$, complexes will also be formed in the matrix, but are of no consequence. Each of these $3\text{HF}\cdot(\text{solvent})_n$ complexes will have its own characteristic emission and excitation spectrum. Thus, as diffusion proceeds new features will appear in both the emission and excitation spectra. Analysis of the appearance kinetics of each spectral feature during the annealing process can establish the stoichiometry of the complex giving rise to that spectral feature. Complexes can be formed with many solvents such as H_2O , MeOH , EtOH , ether, etc. 3HF diffusion remains quite slow below 32 K and 3HF dimers are not formed. Annealing of pure 3HF/Ar matrices results in little or no change in the spectra.

Some 3HF/solvent/Ar matrices were deposited at 30 K producing $3\text{HF}\cdot(\text{solvent})_n$ complexes during deposition. Variation of the argon:solvent ratio results in changes of the relative intensities of the different complex spectral features. Analysis of these results also permits the determination of complex stoichiometries. In all cases the 30 K dilution studies and annealing kinetic studies result in the same conclusions.

The dispersed emission spectra of $3\text{HF}\cdot(\text{MeOH})_n$, $n = 0, 1, 2$, complexes are shown in Figure 4. Analysis of the appearance kinetics establishes the stoichiometry of the complex giving rise to the new 420- and 495-nm spectral features. This analysis is complicated by the polycrystalline nature of the matrix. Diffusion readily occurs along crystal grain boundaries and defects, and much more slowly through the microcrystals. As a result, the diffusion process cannot be characterized by a single diffusion constant. Furthermore, each individual matrix has slightly different diffusion properties. Despite these difficulties, complex stoichiometries can be unambiguously determined in most cases. Several predictions about the appearance kinetics are insensitive to the specifics of the diffusion process. These predictions are simplified by the assumptions that the solvent concentration is much larger than the 3HF concentration and that the solvent dimer diffusion rate is much slower than that of the solvent monomer. The first assumption is justified by the known matrix deposition conditions, and the second by the observation that the larger solvents (e.g., MeOH , EtOH , or Et_2O) diffuse much slower than H_2O or D_2O . We predict that the first complex to appear in significant amounts is the monosolvate. The concentration of monosolvate should initially increase linearly with time, and at later times levels off. We also predict that, with a single diffusion coefficient, the disolvate concentration should initially increase quadratically with time and eventually level off. The distribution of diffusion coefficients inherent to the polycrystalline matrix results in more complicated kinetic behavior, particularly for the disolvate. The distribution of diffusion coefficients is unknown, and no quantitative predictions can be made. However, irrespective of the distribution of diffusion coefficients, the disolvate/monosolvate ratio should increase monotonically with time.

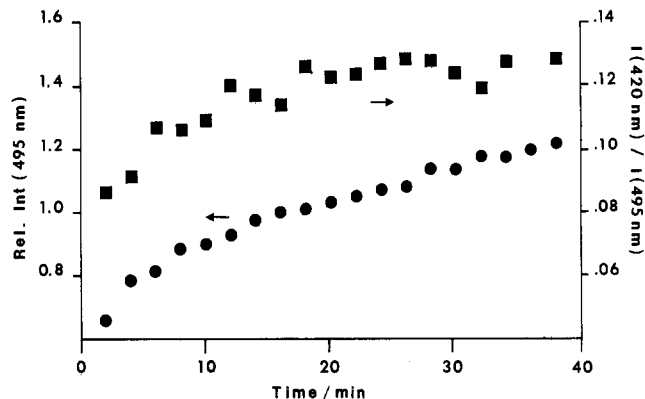


Figure 5. Experimental plots of (A) 495-nm emission intensity and (B) 420-nm/495-nm emission intensity as a function annealing time. These data are for $3\text{DF}/\text{D}_2\text{O}/\text{Ar}$. The Ar: D_2O ratio was 2000:1.

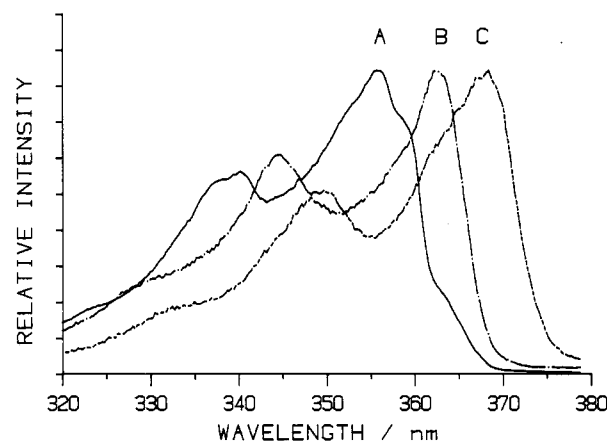


Figure 6. Fluorescence excitation spectra under the conditions of Figure 4, taken at (A) 515, (B) 495, and (C) 420 nm.

This ratio initially increases linearly with time and eventually levels off. The kinetics of the 495-nm emission intensity and of the 420 nm/495 nm emission intensity ratio are shown in Figure 5. These kinetics are qualitatively in accord with the above predictions, establishing the assignments in Figure 4. McMorrow and Kasha⁶ have previously observed analogous spectral bands in wet hydrocarbon solutions. Dilution studies permit the assignment of stoichiometries under these conditions. The assignments in Figure 4 are consistent with those of ref 6.

Figure 4 shows that the intensity of monosolvate emission is a factor of 5–10 lower than that of the unsolvated molecule. Furthermore, the disolvate (normal) emission intensity is a factor of ~ 10 lower than monosolvate emission intensity. These observations indicate that under the matrix annealing conditions used in these studies, only about 10–20% of the 3HF is solvated. The low intensity of normal emission indicates that the concentration of $3\text{HF}\cdot(\text{solvent})_2$ complexes is quite low, about 1–2% of the total. We conclude that the concentration of $3\text{HF}\cdot(\text{solvent})_n$, $n > 2$, is negligible (0.1–0.2% of the total).

2. 3HF Water and Alcohol Monosolvates. Figure 4 shows that most of the monosolvate emission spectrum is buried under that of the unsolvated molecule. However, it is possible to selectively excite the solvated molecules. $3\text{HF}/\text{MeOH}/\text{Ar}$ excitation spectra observing at 515, 495, and 420 nm are shown in Figure 6. These wavelengths correspond to emission from nonsolvate, monosolvate, and disolvate 3HF, respectively. The $3\text{HF}\cdot(\text{MeOH})_1$ excitation spectrum is shifted to longer wavelengths compared to the unsolvated 3HF. A further red shift is observed in the $3\text{HF}\cdot(\text{MeOH})_2$ complex. Figure 6 shows that irradiation at wavelengths in the 370–376-nm region excites predominately the disolvate complexes. Similarly, 362–376-nm light excites both mono- and disolvate complexes, but not the unsolvated 3HF molecule. Figure 7 shows the dispersed emission spectra following 365- and 370-nm irradiation. No unsolvated 3HF emission is

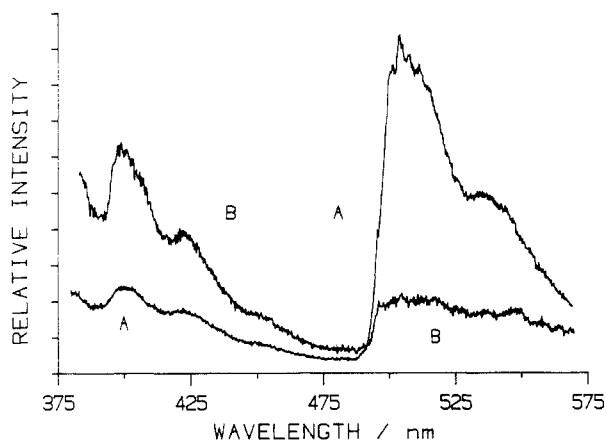


Figure 7. Dispersed emission spectra of 3HF/MeOH/Ar under the same conditions as Figure 4 with irradiation of (A) 365 and (B) 370 nm.

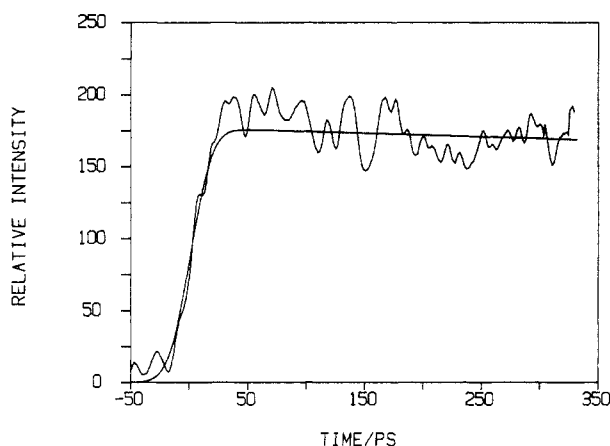
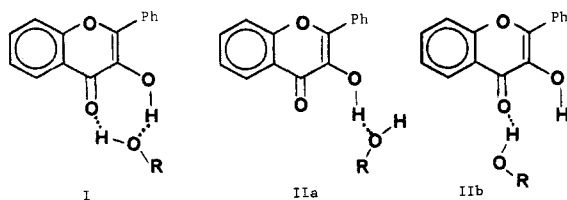


Figure 8. Emission kinetics of the 3HF·(MeOH)₁ complex following 364-nm picosecond excitation. The observation wavelength was 495 ± 2 nm. Also shown is a calculated curve corresponding to the convolution of the instrument response function and a fast risetime.

observed. The 490–575-nm band in Figure 6A corresponds to the slightly blue-shifted 490-nm shoulder seen in Figure 4 and is therefore also assigned to the 3HF·(MeOH)₁ complex. As in Figure 4, the normal (375–450-nm) emission seen in Figure 7 is assigned to disolvate complexes. Very similar results were obtained with ethanol complexes at slightly higher (~30 K) annealing temperature and water complexes at lower (~26 K) annealing temperatures. The excitation spectra of water complexes are very slightly blue shifted with respect to those of the methanol complexes.

Figure 6 shows that methanol-solvated 3HF can be selectively excited by 364-nm light. 495 ± 2 nm emission kinetics under conditions corresponding to Figure 4, and following 364-nm picosecond excitation are shown in Figure 8. This spectral region corresponds to the blue edge of the 3HF·(MeOH)₁ emission spectrum. The kinetics show that monosolvate tautomeric emission appears rapidly (<10 ps) following photoexcitation.

There has been some discussion regarding the nature of the species giving rise to the 490–575-nm emission observed in wet hydrocarbon solutions. Sengupta and Kasha² originally assigned this to a cyclically hydrogen-bonded 3HF tautomer formed by ESPT of I. More recently, McMorrow and Kasha⁶ reassigned

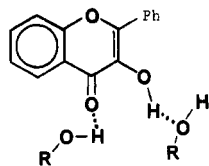


the peak to the 3HF anion, formed by intermolecular (3HF to

solvent) proton transfer to water clusters. The nature of the water cluster hydrogen bonding to 3HF is analogous to that shown in IIa, i.e., hydrogen bonding only to the 3HF OH group. Although it seems somewhat unlikely that a single solvent molecule could stabilize the 3HF anion, we need to establish the nature of the monosolvate species (3HF anion or tautomer) observed here. Analysis of the high-resolution 3HF·H₂O and 3DF·D₂O dispersed emission spectra along with time-resolved results can resolve this tautomer vs. anion ambiguity. The ground-state tautomeric 3HF is largely zwitterionic. We therefore expect that solvation will stabilize the ground with respect to the excited state and will blue shift the tautomeric emission as observed. Furthermore if the 490–575-nm emitting species is the 3HF anion, then it is expected that hydroxyl deuteration would have little or no effect on the spectra or emission lifetime. The 3HF·H₂O and 3DF·D₂O spectra are slightly different (spectral shifts of a few wavenumbers), also suggesting that the luminescent species is a tautomer rather than the anion. However, it could be argued that the spectra are from 3HF anions and the spectral differences result from hydrogen bonding to H₃O⁺ and D₃O⁺. Time-resolved results show that deuteration also has a dramatic effect on the 495-nm emission lifetime. For example, the 3HF·MeOH and 3DF·MeOD 495-nm emission lifetimes are about 7 and 13 ns, respectively. It is quite unlikely that small changes in the hydrogen-bonding environment (deuteration) would result in such a large effect on the emission lifetime. These observations therefore support the assignment of the 490–575-nm emission to a monosolvated tautomer.

The above result allows us to comment on the monosolvate structure and ESPT mechanism. The 3HF–solvent complexes are formed at a temperature that is never greater than 30 K. Under these conditions we can expect energetic factors to determine the configuration of the complexes that are formed. The double hydrogen-bond present in I provides stability compared to the singly hydrogen-bonded IIa and IIb. Thus, a cyclically hydrogen-bonded structure (I) would therefore be the most energetically stable configuration and would predominate at low temperature. Rapid (<10 ps) ESPT is also consistent with monosolvate structure I. ESPT can occur without rupture of hydrogen bonds that would be required for ESPT to occur in IIa and IIb. The possibility of having monosolvates where the solvent molecule is hydrogen bonded to the ether group is unlikely because of the steric interference that exists with the phenyl ring. The fact that the monosolvate tautomer risetime is pulse width limited does not allow us to distinguish between a concerted mechanism or a very fast double proton-transfer mechanism with a short-lived ion pair (3HF anion, RO⁺H₂ cation) intermediate.

3. 3HF Water and Alcohol Disolvates. The diffusion appearance kinetics discussed above establish that the majority of normal emission seen in Figures 4 and 7 is from disolvate complexes. We can conclude that complexation with two methanols at least partially inhibits proton transfer. However, on the basis of the static spectra, it cannot be determined if some relatively small fraction of tautomeric emission is due to disolvate complexes following ESPT. Time-resolved studies clarify this issue. The normal (420 nm Figure 4) emission kinetics from matrix-isolated 3HF·(MeOH)₂ show a 3.2-ns exponential decay. The lack of any detectable 3.2-ns risetime of the tautomeric emission indicates that proton transfer is not a quenching mechanism for disolvate normal emission. Thus, we conclude that 3HF·(MeOH)₁ complexes undergo rapid proton transfer, and that 3HF·(MeOH)₂ complexes undergo no excited-state proton transfer. A structure such as III could explain the absence of proton transfer in disolvate complexes. ESPT would require the breaking and re-formation of hydrogen bonds. The process of breaking and reorganization of hydrogen bonds is highly temperature and viscosity dependent. The 420-nm emission kinetics indicate that these processes do not occur within the lifetime of the normal molecule excited state when the molecules are in a rigid argon matrix at 10 K. While we expect the III → I process to have a considerable activation barrier and therefore be very slow at low temperatures, we also expect this process to speed up considerably at higher temperatures. Solvent reorganization in liquid solutions could result in the formation



III

of cyclically or intramolecularly hydrogen-bonded structures which undergo rapid ESPT. This mechanism may explain the slow risetimes observed in protic solvents.³⁻⁵

The same conclusions were found to hold for both water and ethanol complexes. Apparently, slight changes in hydrogen-bond strength do not dramatically change the ESPT mechanism.

4. 3HF Ether Complexes. Formation of ether complexes has little effect on the static spectra. After extended 30 K annealing, very weak normal (400–450) and 490-nm emissions were detected. These spectra correspond to the $3\text{HF}\cdot(\text{H}_2\text{O})_{1,2}$ spectra and probably result from trace water impurities in the ether. (It must be kept in mind that water diffuses through the matrix very much more readily than a comparatively large molecule such as diethyl ether. Thus, small quantities of water can significantly perturb the spectra in these cases.)

Normal emission from ether complexes can be detected with the streak camera. The normal emission decay kinetics of 3HF/ether complexes are shown in Figure 9. The observed normal emission lifetime and hence proton-transfer time is about 40 ps. Due to the short lifetime and the presence of water impurities this emission cannot be detected by static spectroscopy. We therefore cannot definitely establish the stoichiometry of the complex giving rise to this emission. However, it is plausible that this transient results from a monosolvate $3\text{HF}\cdot(\text{ether})_1$ complex via the mechanism in Scheme II.

The scission of the hydroxyl–ether hydrogen bond and the formation of the intramolecular hydrogen bond probably occur in concert. No temperature-dependent or deuteration studies have been performed, and we cannot say if this is an activated or a tunneling process. However, the fact that the reaction is fast (~ 40 ps) at 10 K suggests that the hydroxyl–ether hydrogen bond is fairly weak, and that reorganization occurs via proton tunneling. No static $3\text{HF}\cdot(\text{ether})$ tautomeric emission spectrum can be detected, implying that ether hydrogen bonding causes only a slight spectral shift with respect to the bare molecule. This observation is also consistent with a fairly weak hydroxyl–ether hydrogen bond.

Conclusions

The main conclusions of this work can be summarized as follows:

Solute–solvent complexes of known stoichiometry can be formed and spectroscopically characterized in rare gas matrices. The spectra of different complexes remain relatively sharp and permit reasonably selective excitation and detection of each species.

Unsolvated 3HF isolated in 10 K argon matrices undergoes rapid (<10 ps) excited-state proton transfer. This is indicated by both static and direct time-resolved measurements.

Static spectroscopic (line width) results indicate that the ground electronic surface has two distinct local minima, corresponding to the normal and tautomeric forms. The line widths can be

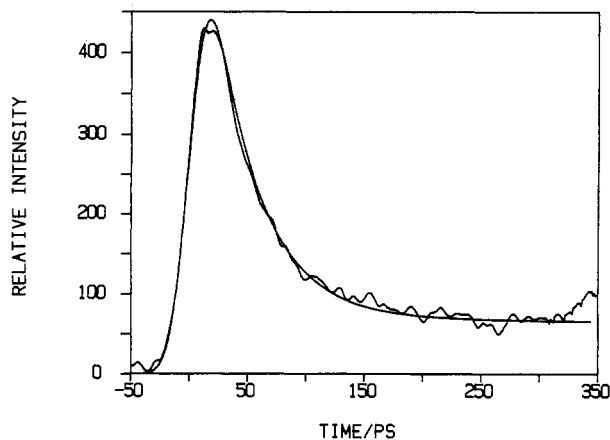
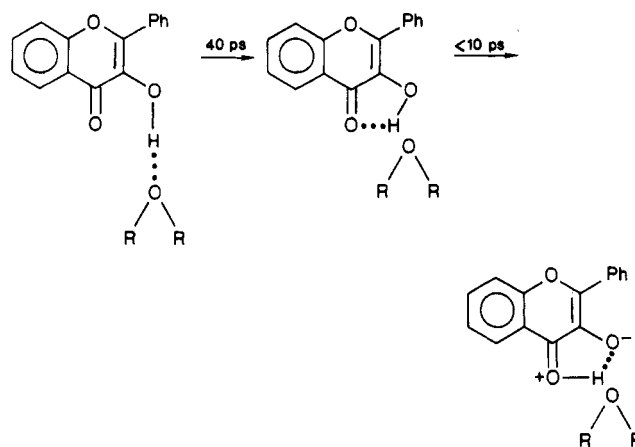


Figure 9. Normal molecule (420 ± 10 nm) emission kinetics obtained following 355-nm picosecond excitation of an annealed 3HF/ Et_2O /Ar matrix. The argon:ether ratio was 2000:1, and the matrix was annealed 15 min at 32 K. Also shown is a calculated curve corresponding to the convolution of the instrument response function, a fast risetime, and a biphasic decay. The decay times are 40 ps and 4.0 ns. The slowly decaying component is probably due to trace water impurities.

SCHEME II



interpreted in terms of rapid (~ 60 fs) reverse proton transfer in the unsolvated molecule.

The $3\text{HF}\cdot(\text{ROH})_1$, $\text{R} = \text{H, Me, T}$, complexes can be selectively excited by 364-nm laser pulses. Time-resolved emission spectroscopy indicates that they undergo rapid (<10 ps) ESPT. This can be interpreted in terms of a cyclic hydrogen-bonded structure that the alcohol or water forms with the hydroxyl and carbonyl groups.

The $3\text{HF}\cdot(\text{Et}_2\text{O})_1$ complex undergoes ESPT in about 40 ps. This process probably requires partial breakage of the comparatively weak hydroxyl–ether hydrogen bond.

Complexation of 3HF to two or more water or alcohol molecules inhibits ESPT at low temperatures. Reorganization of disolvate hydrogen bonds may explain the slow ESPT times observed at higher temperatures.

Acknowledgment. This work was supported by the National Science Foundation.